DEPARTMENT OF THE INTERIOR
UNITED STATES GEOLOGICAL SURVEY

Prepared for the
NATIONAL AERONAUTICS AND SPACE ADMINISTRATION

ATLAS OF MARS
1:5 000 000 GEOLOGIC SERIES
SINUS SABAEUS QUADRANGLE
M SM −15/338 G, 1980
I-1196 (MC-20)

NOTES ON BASE

This map sheet is one of a series covering the entire surface of Mars at nominal scales of 1:25 000 000 and 1:5 000 000 (Batson, 1973, 1976). The major source of map data was the Mariner 9 television experiment (Masursky and others, 1970).

ADOPTED FIGURE

The figure of Mars used for the computation of the map projection is an oblate spheroid (flattening of 1/192) with an equatorial radius of 3393.4 km and a polar radius of 3375.7 km. This is not the height datum which is defined below under the heading "Contours."

PROJECTION

The Mercator projection is used for this sheet, with a scale of 1:5 000 000 at the equator and 1:4 336 000 at lat 30°. Longitude increases to the west in accordance with the usage of the International Astronomical Union (IAU, 1971). Latitudes are areographic (de Vaucouleurs and others, 1973).

CONTROL

Planimetric control is provided by photogrammetric triangulation using Mariner 9 pictures (Davies, 1973; Davies and Arthur, 1973) and the radio-tracked position of the spacecraft. The first meridian passes through the crater Airy-0 (lat 5.9° S) within the crater Airy. No simple statement is possible for the precision, but local consistency is about 10 km.

MAPPING TECHNIQUES

A series of mosaics of Mercator projections of Mariner 9 pictures was assembled at 1:5 000 000.

Shaded relief was copied from the mosaics and portrayed with uniform illumination from the sun to the west. Many Mariner 9 pictures besides those at the time of the mosaics were used to improve the portrayal (Leovitha and others, 1973; Green and others, 1973; Inge and Bridges, 1976). The shading is not generalized and may be interpreted with nearly photographic reliability (Inge, 1972).

Shaded relief analysis and representation were made by Barbara J. Hall.

CONTOURS

Because Mars has no seas and hence no sea level, the datum (the 0 km contour line) for altitudes is defined by a gravity field described by spherical harmonics of fourth order by a gravity field described by spherical harmonics of fourth order by a gravity field described by Lorell, 1973) combined with a 6.1-millibar atmospheric pressure surface derived from radio-occultation data (Kliore and others, 1972; Christeensen, 1975; Wu, 1975; Fjeldbo, 1976).

The contour lines on most of the Mars maps (Wu, 1975; 1978) were compiled from Earth-based radar determinations (Downs and others, 1973; Pettengill and others, 1973) and measurements made by Mariner 9 instrumentation, including the ultraviolet spectrometer (Hord and others, 1974), infrared interferometer spectrometer (Conrath and others, 1973), and stereoscopic Mariner 9 television pictures (Wu and others, 1973).

Formal analysis of the accuracy of topographic elevation information has not been made. The estimated vertical accuracy of each scarce of data indicates a probable error of 1-2 km.

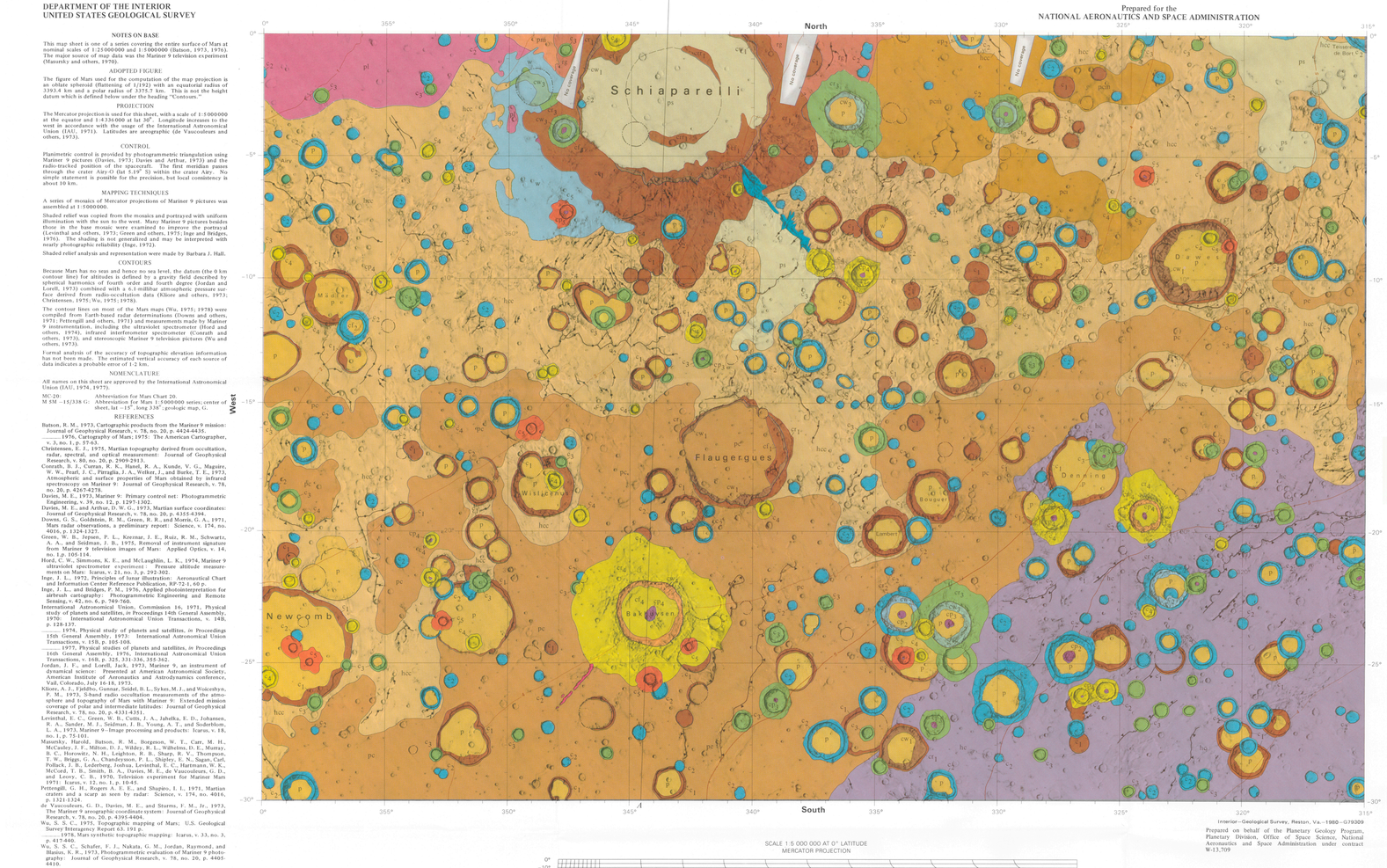
NOMENCLATURE

All names on this sheet are approved by the International Astronomical Union (IAU, 1974, 1977).

MC-20 Abbreviation for Mars Chart 20.
M SM −15/338 G: Abbreviation for Mars 1:5000000 series: center of sheet, lat −15° long 338° geologic map, G.

REFERENCES

Batson, R. M., 1973, Cartographic products from the Mariner 9 mission: Journal of Geophysical Research, v. 78, no. 20, p. 4424-4435.
———1976, Cartography of Mars; 1975: The American Cartographer, v. 3, no. 1.
Christensen, E. J., 1975, Martian topography derived from occultation, radar, spectral, and optical measurement: Journal of Geophysical Research, v. 80, no. 20, p. 2909-2913.
Conrath, B. J., Curran, R. K., Hanel, R. A., Kunde, V. G., Maguire, W. W., Pearl, J. C., Pirraglia, J. A., Welker, J., and Burke, T. E., 1973, Atmospheric and surface properties of Mars obtained by infrared spectroscopy on Mariner 9: Journal of Geophysical Research, v. 78, no. 20, p. 4267-4278.
Davies, M. E., 1973, Mariner 9: Primary control net: Photogrammetric Engineering, v. 39, no. 12, p. 1297-1302.
Davies, M. E., and Arthur, D. W. G., 1973, Martian surface coordinates: Journal of Geophysical Research, v. 78, no. 20, p. 4355-4394.
Downs, G. S., Goldstein, R. M., Grieg, R. R., and Morris, G. A., 1971, Mars radar observations, a preliminary report: Science, v. 174, no. 4016, p. 1324-1327.
Green, W. B., Jepsen, P. L., Kreznar, J. E., Ruiz, R. M., Schwartz, A. A., and Seidman, J. B., 1975, Removal of instrument signature from Mariner 9 television images of Mars: Applied Optics, v. 14, no. 1,p. 105-114.
Hord, C. W., Simmons, K. E., and McLaughlin, L. K., 1974, Mariner 9 ultraviolet spectrometer experiment: Engineering and altitude measurements: Icarus, v. 23, p. 392-402.
Inge, J. L., 1972, Principles of lunar illustration: Aeronautical Chart and Information Center Reference Publication, RP-72-1, 69 p.
Inge, J. L., and Bridges, P. M., 1976, Applied photointerpretation for airbrush cartography: Photogrammetric Engineering and Remote Sensing, v. 42, no. 6, p. 749-760.
International Astronomical Union, Commission 16, 1971, Physical study of planets and satellites, *in* Proceedings 14th General Assembly, 1970: International Astronomical Union Transactions, v. 14B, p. 128-135.
———1974, Physical study of planets and satellites, *in* Proceedings 15th General Assembly, 1973: International Astronomical Union Transactions, v. 15B, p. 105-108.
———1977, Physical studies of planets and satellites, *in* Proceedings 16th General Assembly, 1976: International Astronomical Union Transactions, v. 16B, p. 325, 331-336, 355-362.
Jordan, J. F., and Lorell, Jack, 1973, Mariner 9, an instrument of dynamical science: Presented at American Astronautical Society, American Institute of Aeronautics and Astrodynamics conference, Vail, Colorado, July 30-August 1, 1973.
Kliore, Arvydas, Fjeldbo, Gordon, Seidel, B. L., Sykes, M. J., and Woiceshyn, P. M., 1973, S-band radio occultation measurements of the atmosphere and topography of Mars with Mariner 9: Extended mission coverage of polar and intermediate latitudes: Journal of Geophysical Research, v. 78, no. 20, p. 4331-4351.
Leovitha, E. C., Green, W. B., Cutts, J. A., Jahelka, E. D., Johansen, R. A., Sander, M. J., Seidman, J. B., Young, A. T., and Soderblom, L. A., 1973, Mariner 9—Image processing and products: Icarus, v. 18, no. 1, p. 75-101.
Masursky, Harold, Batson, R. M., Borgeson, W. T., Carr, M. H., McCauley, J. F., Milton, D. J., Wildey, R. L., Wilhelms, D. E., Murray, B. C., Horowitz, N. H., Leighton, R. B., Sharp, R. V., Thompson, T. W., Briggs, G. A., Chandeysson, P. L., Shipley, E. N., Sagan, Carl, Pollack, J. B., Lederberg, Joshua, Leventhal, E. C., Hartmann, W. K., McCord, T. B., Smith, B. A., Davies, M. E., de Vaucouleurs, G. D., and Levoy, C. B., 1970, Television experiment for Mariner Mars 1971: Icarus, v. 12, no. 1, p. 10-45.
Pettengill, G. H., Rogers A. E., and Shapiro, I. I., 1971, Martian craters and a scarp as seen by radar: Science, v. 174, no. 4016, p. 1328-1331.
de Vaucouleurs, G. D., Davies, M. E., and Sturms, F. M., Jr., 1973, The Mariner 9 areographic coordinate system: Journal of Geophysical Research, v. 78, no. 20, p. 4395-4404.
Wu, S. S. C., 1975, Topographic mapping of Mars: U.S. Geological Survey Interagency Report 63, 191 p.
———1978, Mars synthetic topographic mapping: Icarus, v. 33, no. 3, p. 417-446.
Wu, S. S. C., Schafer, F. J., Nakata, G. M., Jordan, Raymond, and Blasius, K. R., 1973, Photogrammetric evaluation of Mariner 9 photography: Journal of Geophysical Research, v. 78, no. 20, p. 4405-4410.



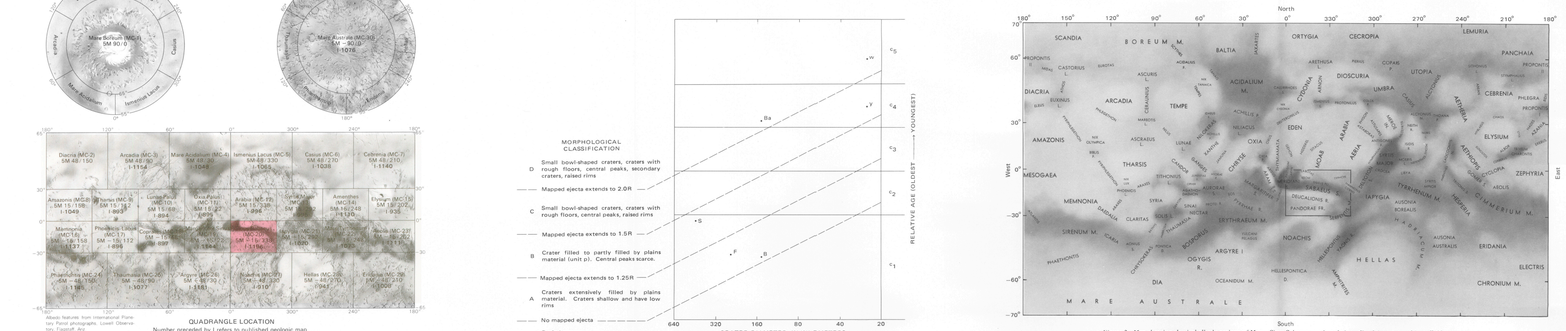


Figure 1. *System used to assign relative ages of craters. Morphologies of individual craters were determined first, then ages were determined according to their size and superposition relations. Youngest craters are* c_0 *and oldest craters* c_5*. Ba indicates classification of Bakhuysen; B, Bouguer; S, Schiaparelli; F, Flaugergues; w and y two small craters. R is one crater radius, so that 2.0R means ejecta of crater extend two crater radii from center of crater. See discussion in description of map units.*

Figure 2. *Map showing classical albedo regions of Mars. Sinus Sabaeus quadrangle is outlined (courtesy of Lowell Observatory).*

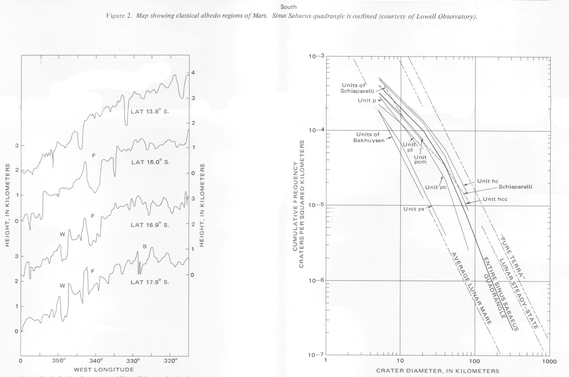


Figure 3. *Relief in the region of Sinus Sabaeus obtained from radar observations (Downs and others, 1973). Note that smoothed surface forms a broad ridge at lat 16.9° S. and 17.9° S. and local relief is near 1.3 km. F, crater Flaugergues; W, crater Wislicenus; B, crater Bouguer.*

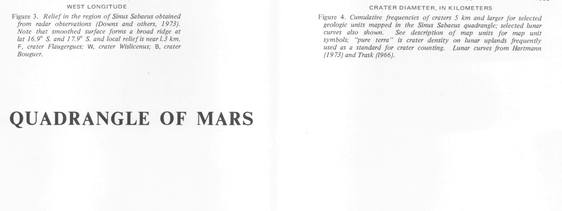


Figure 4. *Cumulative frequencies of craters 5 km and larger for selected geologic units mapped in the Sinus Sabaeus quadrangle; selected lunar curves also shown. See description of map units for map unit symbols; "pure terra" is crater density on lunar uplands frequently used as a standard for crater counting. Lunar curves from Hartmann (1973) and Trask (1966).*

SCHEMATIC CROSS SECTION

Cross section extends beyond north boundary of Map in order to depict the rim of Schiaparelli. Small and subdued craters have been omitted. Equal intervals between parallels of latitude.

CORRELATION OF MAP UNITS

CRATER MATERIALS	PLAINS FORMING MATERIALS	OTHER MATERIALS
c_0		
cf_0 c_4	cw_4 c_4	
cf_4 cw_4 c_4	cw_4 c_4	
cf_3 cw_3 c_3	cw_3 c_3	c_4
cf_2 cw_2 c_2	cw_2 c_2	p ps
cf_1 cw_1 c_1	cw_1 c_1	pm pcm pc
cf_0 cw_0 c_0	cw_0 c_0	w
		rg
		hcc
		hc

DESCRIPTION OF MAP UNITS

CRATER MATERIALS (CRATERS ≥ 20-KM DIAMETER)

Craters of ≥ 20-km diameter were mapped and assigned relative ages using a system based on both morphology and size (fig. 1) because crater lifetimes affected by both erosion and infilling increase with crater size. Craters were first classified by their morphology and the extent of mappable ejecta, then assigned a relative age according to size and superposition relations with other craters (fig. 1). These data were used to construct the morphology chart of figure 1. Craters designated as c_5 are the youngest, those designated c_1 the oldest. By this system, craters between 20 and 30 km must be c_4 or younger. Craters larger than 30 km can have any age, depending on their morphology, extent of ejecta, and size. The crater Bakhuysen (lat 23° S., long 344° W.; Ba in fig. 1) is a c_4 crater and relatively young because its mapped ejecta extend beyond two crater radii from the crater center and it has a central peak, fairly rough crater-floor material, and satellitic craters. The crater Bouguer (lat 18° S., long 326° W.; B in fig. 1), about the same size as Bakhuysen, is a c_3 crater and relatively old because its floor is filled and its flanks are narrow and smooth. The smaller crater (lat 25.5° S., long 343° W.; w in fig. 1) on the ejecta of Bakhuysen is a c_2 crater and young because its ejecta extend beyond two crater radii from the center of the crater and it is near 25 km across. A crater northeast of Bakhuysen (lat 19.2° S., long 339° W.; y in fig. 1) is a c_4 and in the same age group as Bakhuysen because its mapped ejecta extend 1.7 crater radii from its center and it is 25 km across. The positions of the basin Schiaparelli and the filled crater Flaugergues (lat 16°S., long 341°W.) are indicated by S and F in figure 1

MATERIAL OF YOUNGEST CRATERS–Well-preserved small craters typically 20 to 30 km across, with prominent raised rim and evidence of roughness on crater flanks. Central-peak material (cp_4) common. *Interpretation:* Among young craters and their ejecta of crushed rock and large blocks

MATERIAL OF YOUNG CRATERS–Well-preserved craters larger than about 30 km across with prominent raised rim, rough crater flanks and crater floor; crater-rim (cf_4), crater-floor (cf_4), crater-wall (cw_4) and central-peak (cp_4) (where present) materials are mapped on large craters. Smaller craters have distinct raised rims and some evidence for roughness on flanks. *Interpretation:* Young impact craters and their ejecta modified by eolian and other processes to a greater extent than c_4 craters

MATERIAL OF INTERMEDIATE-AGE CRATERS–Largest craters are well preserved and have raised rim; crater flanks and floor appear more subdued and less extensive than those of c_4 craters; craters partly filled by plains material (p), may have central peaks; crater-rim (cf_3), crater-floor (cf_3), crater-wall (cw_3), and central-peak (cp_3) (where present) materials are mapped in larger craters. Small craters are moderately well preserved but may be partly filled. *Interpretation:* Impact craters and their ejecta that have been modified by eolian and impact-cratering processes

MATERIAL OF OLD CRATERS–Large craters that have smooth planar interior surfaces and narrow flanks; crater-rim (cf_2), crater-wall (cw_2), and crater-floor (where present) (cf_2) materials mapped in larger craters. Small craters, 20 to 30 km across, shallow with level planar floors are subdued. *Interpretation:* Impact craters and their ejecta eroded and filled by eolian, impact, fluvial, and possibly volcanic processes

MATERIAL OF OLDEST CRATERS–Very shallow craters larger than 30 km across with smooth planar interior surfaces; crater rim subdued and crater flanks narrow; crater rim may be absent in some sectors. Crater-rim (cf_1), crater-wall (cw_1), and crater-floor (cf_1) (where present) materials mapped on large craters. Large crater in Sinus Sabaeus, Sinus Meridiani, and Serpentin Minor (fig. 2), high thermal inertias and low albedos; (3) Small craters, 5 to 20 km across, have high thermal inertias and moderate albedos. Thermal inertias greater than 5 cov roughly half the quadrangle suggest concentrations of rocks, wet or dry ice, or both, comparable to concentrations in the immediate vicinity of Viking landing sites (about 20 percent of the area covered by rocks, Moore and others, 1977); but other models are possible (Kieffer and others, 1977).

PREVIOUS WORK

Generalized geologic mapping of Mars, including the entire area of the Sinus Sabaeus quadrangle as undivided crater materials (Carr and others, 1973). Subsequent generalized geologic mapping of Mars (Carr and others, 1977; Pig. 1978) recognized six units: (1) plains, (2) ridged plains, (3) cratered plateau, (4) knobby, (5) basin rim, and (6) hilly and cratered materials. Larger quadrangles at 1:5 000 000 scale delineated by crater counts and classified most of the area as moderately cratered plains (McCauley and others, 1972). Most of the quadrangle was classified as Intermediate terrain in the northwest quarter by Schiaparelli (Edom) was recognized. Other units recognized were densely cratered terrain mapped as patches concentrated in the northwest corner of the quadrangle contains more than one crater per 10^5 km^2 (Hartmann, 1973). Crater densities for the rest of the quadrangle are between 5 and 10 per 10^5 km^2. At this scale, the area is densely cratered. Densities of craters larger than 20 km show a more complex pattern than craters larger than 64 km (Soderblom and others, 1974). The lowest density of craters larger than 20 km is in the northwest corner of the quadrangle, where less than 5 percent of the area is covered by craters larger than 20 km. In the eastern part generally, 15 to 35 percent of the area is covered by craters larger than 20 km; a band of this concentration of craters extends northwestward across the western part of the quadrangle from lat 25° S., long 345° W. to lat 10° S. and long 330° W. Concentrations of craters 4-10 km across are lowest in the northwest near Schiaparelli (about 45 per 10^6 km^2), and usually larger concentrations are found in the southwest corner of the quadrangle (about 220 per 10^6 km^2; Soderblom and others, 1974). Concentrations of craters 0.4-1.2 km across are lowest in the northwest corner of the map area (< 1500 per 10^6 km^2) near Schiaparelli and highest in the south half of the quadrangle (> 6000 per 10^6 km^2). These cratered data, then, suggest that the units in the northwest corner are relatively younger than those in the southeast corner of the map area; the units in the rest of the map area are somewhere between these two extremes.

PICTURE QUALITY

Mariner 9 arrived to orbit Mars during the 1971 dust storm (Cutts, 1974, p. 6-10). Initially, at the time the A-frame pictures were taken, most of the surface of Mars was obscured by dust and haze; clearing of the planet was a function of time, areographic location, and elevation. With time, atmospheric clearing proceeded from south to north and from higher to lower elevations. Even with the general clearing of the atmosphere, local surfaces were partly obscured by haze, dust, and transient deposits of fine materials. Several episodes of surface visibility occur in the southeast and northwest corners and within Schiaparelli. Pictures obtained of the west edge of Sinus Sabaeus during the Viking Mission (Snyder, 1977) show by comparison that atmospheric obscuration was extensive in the Sinus Sabaeus quadrangle during the Mariner 9 mission. In addition, surface resolutions of the Viking pictures are higher. Revisions of map units and geologic interpretations for this quadrangle are expected.

Mariner 6 obtained pictures of part of Sinus Sabaeus (National Aeronautics and Space Administration, 1971). In some pictures, some features can be seen more clearly than in the Mariner 9 pictures; in other pictures, features cannot be seen as clearly. In no case is resolution of Mariner pictures as good as that of pictures taken by the Viking Orbiters.

GEOLOGIC SUMMARY

The area included in the Sinus Sabaeus quadrangle represents an ancient cratered surface that has been modified by a combination of impact cratering, fluvial, eolian, and, probably, volcanic processes. Impact cratering has been the dominant process. Cumulative frequencies of craters larger than 20 km for the entire quadrangle (fig. 4) are only about a factor of two below the idealized lunar steady-state curve (Moore, 1964; Trask, 1966). Two of the units mapped (hilly, channeled, and cratered material and hilly and cratered material) have cumulative frequencies of craters larger than 40 km that are nearly the same as the idealized steady-state curve. The young map units (smooth plains material and units of the crater Bakhuysen) have cumulative frequencies of craters and distributions that are similar in form and magnitude to the average frequency distributions of lunar maria. Ages of surfaces recorded by craters larger than 5 km (fig. 4) are probably measured in several billions of years. Direct comparison with lunar craters would place the age of the young units (smooth plains material and units of Bakhuysen) in the range 3.2 to 3.5 billion years, but procedures for making such a comparison are controversial. (See, for example, Soderblom and others, 1974; Neukum and Wise, 1976). These units may be either a few tenths of a billion years older or about a billion years younger than the average lunar maria. The more cratered units (hilly, channeled, and cratered material and hilly and cratered material) may represent the cumulative result of about 4 billion years of cratering (Soderblom and others, 1974; Neukum and Wise, 1976).

For most surfaces, in figure 4, the frequency distribution of craters deviates from the lunar curve. For the more cratered map units, this deviation begins at crater diameters near 40 km and in most marked for craters below 20 km, where the slope of the distribution curve is near minus one. Curves of this form have been noted (Soderblom and others, 1974; Neukum and Wise, 1976) and later confirmed from data obtained in pictures taken by the Viking Orbiters (Masursky and others, 1977). Such frequency distributions have been generally attributed to resurfacing (Neukum and Wise, 1976) by erosion or infilling and degradation (Masursky and others, 1977). They may also represent the result of primary impacts (Soderblom and others, 1974) or steady-state surfaces for which the primary distribution coefficient is slightly less than minus two or for which the lifetime of craters is a suitable function of their size. (See, for example, Moore, 1964). The crater-frequency distributions of Bakhuysen units and smooth-plains material suggest that the crater production curve does in fact have a slope near minus two and that the lower slope of the Soderblom Shoemaker, E. M., 1960, Penetration mechanics of high-velocity meteorites, illustrated by Meteor Crater, Arizona: International Geological Congress, 21st, Copenhagen 1960, Report, Part 18, 418-434.
Snyder, C. W., 1977, The missions of the Viking Orbiters: Journal of Geophysical Research, v. 82, p. 3971-3983.
Soderblom, L. A., Condit, C. D., West, R. A., Herman, B. M., and Kreidler, T. J., 1974, Martian planetwide crater distributions: Implications for geologic history and surface processes: Icarus, v. 22, p. 239-263.
Strom, R. G., 1964, Analysis of lunar lineaments I: Tectonic maps of the Moon: Arizona University Lunar and Planetary Laboratory Communications, v. 2, no. 39, p. 205-216.
Trask, N. J., 1966, Size and spatial distribution of craters estimated from the Ranger photographs, *in* Ranger VIII and IX, Part 2, Experimenters' analyses and interpretations: California Institute of Technology, Jet Propulsion Laboratory Technical Report 32-800, p. 252-264.
U. S. Geological Survey, 1976, Topographic map of Mars: U. S. Geological Survey Miscellaneous Investigations Series Map I-961, scale 1:25 000 000 at 0° latitude.
Van Dorn, W. G., 1968, Tsunamis on the Moon?: Nature, v. 220, p. 1102.
———1969, Lunar maria: structure and evolution: Science, v. 165, p. 693.

into three categories using cumulative frequencies of craters larger than 5 km: (A) young, (B) intermediate, and (C) old. The age of Schiaparelli is assigned to category B on the basis of stratigraphic evidence and the frequency of craters larger than 10 km: the unusually large number of craters 5-10 km across is attributed to secondary impact cratering (Soderblom and others, 1974). Plains materials that fill craters vary widely in age, depending on the age of the craters filled.

Structure

Structural features within the quadrangle are of four types: (1) large graben with irregular boundaries, (2) multiring basins, (3) craters, and (4) reticulate joint patterns. Large graben are concentrated in hilly and cratered material in the southeastern part of the quadrangle, but the largest, which measures about 100 km across, is southeast of Bakhuysen in cratered plains material. The irregular forms of the scarps are produced by faults transecting craters and partial burial by materials filling the graben. Traces of scarps concentric with the rim of the Hellas basin can be traced from the Noachis quadrangle (Peterson, 1977) at lat 42° S., long 340° W., through the southeast corner of the Sinus Sabaeus quadrangle to the west flank of Huygens in the Iapygia quadrangle (Schaber, 1977). It appears likely that these graben are related to the formation and subsequent deformation of the Hellas basin. Scarps concentric to the Isidis basin are similar (Meyer and Grolier, 1977; Schaber, 1977).

Multiringed basin structures are represented by Schiaparelli. Like the lunar basin Schrodinger (Hartmann and Kuiper, 1962; Hartmann and Wood, 1971), Schiaparelli has a central ring that is about half the diameter of its rim, which is slightly larger in an east-west direction than in a north-south direction. A number of hypotheses have been advanced to account for the origin of multiring basins. The central ring may represent the rim of a transient impact crater that has collapsed by slumping (Moore and others, 1974). In this model, Schiaparelli had a raised rim 6.3 km high, a depth below the rim crest of 43 km, and a rim-crest diameter of about 240 km. Within a very short interval of time, a matter of hours after impact of a moonlet, the rim and flanks collapsed inward, producing the central ring and a circular scarp 520 km across. The central ring is then ejecta and fallout some 4.8 km thick underlain by tilted target material. The mapped rim is made of about 0.5 km of ejecta overlying target material tilted gently outward.

Another possible model requires the interaction of shock and stress waves generated by the impact of a moonlet with a relatively strong interface at depth (Oberbeck and Quaide, 1967; Quaide and Oberbeck, 19680. In this model, the central ring becomes a surface expression of a relatively strong interface that has been uplifted (Hodges and Wilhelms, 1978) and is veneered with fallback and impact melt. By analogy with lunar basins, melt and fallback would occur within the central ring and between the rim and ring. Ejecta would occur on the uplifted rim and flanks.

An early concept suggests that target materials within the craters have been uplifted to produce a central ring and peaks by gravitational recoil (Gilbert, 1893) and elastic rebound of shock-compressed target material (Milton and Roddy, 1972). An alternative hypothesis suggests that the rims are "frozen" body waves generated during impact (Van Dorn, 1968; 1969).

A possible structural profile through Schiaparelli shown in the cross section is fashioned after the Ries basin, Germany (Pohl and others, 1977). A strong substrate has been uplifted to produce the central ring. The center is brecciated substrate overlain by dense dacitic and melted debris. Outward from the ring, faulted outward-dipping units are target material overlain by ejecta. The outermost rim is delineated by the outermost scarps. Beyond the scarps are more ejecta.

Structures related to craters include central peaks, structurally uplifted rims, and faults related to slumping. Structural uplift beneath rims of impact craters and faulting and slumping of crater walls are well established (Shoemaker, 1960). Central peaks have been attributed to rebound during decompression of shocked rocks (Milton and Roddy, 1972), gravitational rebound (Gilbert, 1893), and interaction of shock waves with a strong horizontal interface at depth (Oberbeck and Quaide, 1967). The central peaks, which passes through Bakhuysen, shows a possible structural model of a crater.

Reticulate joint are revealed where directions of channels have been controlled by them. They are particularly evident in the hilly, channeled, and cratered material where channels are abundant. Near lat 8° S., long 318° W. indistinct channels was produced particularly distinct diamond-shaped patterns and zig-zag channels with north-northwest and northeast trends. This structural pattern is analogous to the lunar grid (Strom, 1964).

Channels

Numerous anastamosing and dendritic channels are distinctive features of Sinus Sabaeus and other regions of Mars not common to the Moon. Unlike most lunar rilles, these channels commonly form dense radial patterns on crater flanks and walls and are broad and shallow, yet without levees. Some channels have anastomosing patterns (Sagan and others, 1973) as well as terraced walls. Analyses of data returned by the Viking Landers show that significant amounts of water are present in the martian regolith (Biemann and others, 1977) and that the outgassing of Mars must have included large amounts of water, equivalent to a layer with a depth of 10 m over the entire planet (Owen and others, 1977); the north polar cap contains water ice (Kieffer and others, 1977). It seems reasonable to assume that the channels were produced by fluvial erosion. The behavior of the channels and their distribution is somewhat puzzling. Large channel systems with northeasterly trends are common. Surfaces between craters in the southwestern and central parts of the quadrangle (classical areas of Deucalionis Regio and Fastigium Aryn; fig. 2) appear relatively smooth and planar except for incised channels on some of the rougher terrain. Isolated patches of smooth plains material occur among the northern part of the quadrangle (classical areas of Typhon, Edom, and Fastigium Aryn; fig. 2).

Terrestrial-based radar echoes provide some information on local relief (Pettengill and others, 1971; Downs and others, 1973) and surface roughness (Downs and others, 1973). Radar-range measurements were made along four traces corresponding to lat 17.9° S., 16.9° S., 16.0° S. and 13.8° S. The traces cross a number of craters (fig. 3). Maximum relief indicated is 1.3 km for a partly filled and subdued crater, Wislicenus, 130 km across, at lat 17.9° S., and long 348° W.(W, fig. 3). The filled and subdued crater, Flaugergues, at lat 16° S., long 341° W., has comparable relief (F, fig. 3). Other craters such as Bouguer (B, fig. 3) with a relief of 1 km or less can be identified in the radar profiles. Differences in elevation measured by the radar across the quadrangle are close to 3 to 4 km and are consistent with the contour map (with a 1-km-interval) prepared by the U. S. Geological Survey, 1976).

Broadening of the radar signals in doppler and time delay gives an indication of surface roughness at the fine scale (10-200 radar wavelengths). Scattering widths, a measure of surface roughness (Pettengill and others, 1971; Downs and others, 1973), indicate that the root-mean-square slopes at a scale length of 1.3 to 25 m are usually between 2° and 4° with an average near 3° (Downs and others, 1973); those slopes along the 17.9° S. trace show frequent variations but average near 3.5°. Sinus Sabaeus appears relatively smooth to the radar.

Thermal inertias and albedos measured by the Infrared Thermal Mapper of the Viking Orbiter (Kieffer and others, 1977) suggest that there are three broad categories of surfaces: (1) Edom and other plains in the northwest part of the quadrangle have high inertias and high albedos; (2) Sinus Sabaeus, Sinus Meridiani, and Serpentin Minor (fig. 2), high thermal inertials and low albedos; (3) Small craters, 5 to 20 km across, have high thermal inertias and moderate albedos. Thermal inertias greater than 5 cov roughly half the quadrangle suggest concentrations of rocks, wet or dry ice, or both, comparable to concentrations in the immediate vicinity of Viking landing sites (about 20 percent of the area covered by rocks, Moore and others, 1977); but other models are possible (Kieffer and others, 1977).

PREVIOUS WORK

Generalized geologic mapping of Mars, including the entire area of the Sinus Sabaeus quadrangle as undivided crater materials (Carr and others, 1973). Subsequent generalized geologic mapping of Mars (Carr and others, 1977; Pig. 1978) recognized six units: (1) plains, (2) ridged plains, (3) cratered plateau, (4) knobby, (5) basin rim, and (6) hilly and cratered materials. Larger quadrangles at 1:5 000 000 scale delineated by crater counts and classified most of the area as moderately cratered plains (McCauley and others, 1972). Most of the quadrangle was classified as Intermediate terrain in the northwest quarter by Schiaparelli (Edom) was recognized. Other units recognized were densely cratered terrain mapped as patches concentrated in the northwest corner of the quadrangle contains more than one crater per 10^5 km^2 (Hartmann, 1973). Crater densities for the rest of the quadrangle are between 5 and 10 per 10^5 km^2. At this scale, the area is densely cratered. Densities of craters larger than 20 km show a more complex pattern than craters larger than 64 km (Soderblom and others, 1974). The lowest density of craters larger than 20 km is in the northwest corner of the quadrangle, where less than 5 percent of the area is covered by craters larger than 20 km. In the eastern part generally, 15 to 35 percent of the area is covered by craters larger than 20 km; a band of this concentration of craters extends northwestward across the western part of the quadrangle from lat 25° S., long 345° W. to lat 10° S. and long 330° W. Concentrations of craters 4-10 km across are lowest in the northwest near Schiaparelli (about 45 per 10^6 km^2), and usually larger concentrations are found in the southwest corner of the quadrangle (about 220 per 10^6 km^2; Soderblom and others, 1974). Concentrations of craters 0.4-1.2 km across are lowest in the northwest corner of the map area (< 1500 per 10^6 km^2) near Schiaparelli and highest in the south half of the quadrangle (> 6000 per 10^6 km^2). These cratered data, then, suggest that the units in the northwest corner are relatively younger than those in the southeast corner of the map area; the units in the rest of the map area are somewhere between these two extremes.

PICTURE QUALITY

Mariner 9 arrived to orbit Mars during the 1971 dust storm (Cutts, 1974, p. 6-10). Initially, at the time the A-frame pictures were taken, most of the surface of Mars was obscured by dust and haze; clearing of the planet was a function of time, areographic location, and elevation. With time, atmospheric clearing proceeded from south to north and from higher to lower elevations. Even with the general clearing of the atmosphere, local surfaces were partly obscured by haze, dust, and transient deposits of fine materials. Several episodes of surface visibility occur in the southeast and northwest corners and within Schiaparelli. Pictures obtained of the west edge of Sinus Sabaeus during the Viking Mission (Snyder, 1977) show by comparison that atmospheric obscuration was extensive in the Sinus Sabaeus quadrangle during the Mariner 9 mission. In addition, surface resolutions of the Viking pictures are higher. Revisions of map units and geologic interpretations for this quadrangle are expected.

Mariner 6 obtained pictures of part of Sinus Sabaeus (National Aeronautics and Space Administration, 1971). In some pictures, some features can be seen more clearly than in the Mariner 9 pictures; in other pictures, features cannot be seen as clearly. In no case is resolution of Mariner pictures as good as that of pictures taken by the Viking Orbiters.

GEOLOGIC SUMMARY

The area included in the Sinus Sabaeus quadrangle represents an ancient cratered surface that has been modified by a combination of impact cratering, fluvial, eolian, and, probably, volcanic processes. Impact cratering has been the dominant process. Cumulative frequencies of craters larger than 20 km for the entire quadrangle (fig. 4) are only about a factor of two below the idealized lunar steady-state curve (Moore, 1964; Trask, 1966). Two of the units mapped (hilly, channeled, and cratered material and hilly and cratered material) have cumulative frequencies of craters larger than 40 km that are nearly the same as the idealized steady-state curve. The young map units (smooth plains material and units of the crater Bakhuysen) have cumulative frequencies of craters and distributions that are similar in form and magnitude to the average frequency distributions of lunar maria. Ages of surfaces recorded by craters larger than 5 km (fig. 4) are probably measured in several billions of years. Direct comparison with lunar craters would place the age of the young units (smooth plains material and units of Bakhuysen) in the range 3.